Taylor & Francis
Taylor & Francis Group

Combustion Theory and Modelling

ISSN: 1364-7830 (Print) 1741-3559 (Online) Journal homepage: www.tandfonline.com/journals/tctm20

Efficient treatment of secondary kinetic processes for pre-partitioned adaptive chemistry approaches

Pushan Sharma, Ashish S. Newale & Perrine Pepiot

To cite this article: Pushan Sharma, Ashish S. Newale & Perrine Pepiot (2022) Efficient treatment of secondary kinetic processes for pre-partitioned adaptive chemistry approaches, Combustion Theory and Modelling, 26:6, 1098-1113, DOI: 10.1080/13647830.2022.2111275

To link to this article: https://doi.org/10.1080/13647830.2022.2111275

Combustion Theory and Modelling, 2022
Vol. 26, No. 6, 1098–1113, https://doi.org/10.1080/13647830.2022.2111275

Efficient treatment of secondary kinetic processes for pre-partitioned adaptive chemistry approaches

Pushan Sharma [a*], Ashish S. Newale[a,b] and Perrine Pepiot [a]

[a] *Sibley School of Mechanical and Aerospace Engineering, Cornell University, Ithaca, NY, USA*
[b] *ANSYS Inc., Lebanon, NH, USA*

(*Received 19 April 2022; accepted 25 July 2022*)

Probability Density Function (PDF) methods, which allow for the direct integration of chemical kinetics, are well established to accurately simulate turbulent flames with strong turbulence-chemistry interactions. While adaptive chemistry techniques have been proven effective in reducing the high CPU cost and memory requirements associated with the handling of chemistry in such simulations, performance metrics have mostly been focussed on the primary oxidation pathways converting fuel to major products. In contrast, this work investigates the ability of adaptive techniques, in this case, the pre-partitioned adaptive chemistry (PPAC) approach, to handle secondary kinetics pathways that are parallel, but tightly coupled to the main oxidation process, taking NO_x formation as a case study. PPAC relies on a partitioning of the composition space into a user-specified number of regions, on which specialised reduced models are generated using the Directed Relation Graph with Error Propagation (DRGEP) reduction technique. The direct application of that methodology to a mix of hydrocarbon oxidation and nitrogen-related targets is shown to yield excessively detailed region-specific reduced mechanisms in order to properly capture both the main oxidation and the secondary NO_x formation processes, thereby decreasing the benefits of the adaptive approach. To address this issue, a sequential approach is proposed for the generation of the region-specific reduced mechanisms, in which the primary combustion pathways relevant for each region are identified first, followed by the selective addition, directly at the reduced level, of any secondary pathways relevant for that region using a recently developed build-up technique. This new strategy is assessed in the context of propane combustion in a partially stirred reactor (PaSR) and methane combustion in the Sandia Flame D configuration, demonstrating in both cases the benefits of the sequential approach for reduced model generation.

Keywords: adaptive chemistry; PPAC; DRGEP; building algorithm; LES/PDF

1. Introduction

With recent developments in combustion research, using accurate chemical kinetic models has become essential to simulate multidimensional reactive flow problems. However, accommodating such detailed chemistry in actual computational fluid dynamics (CFD) simulations for realistic fuels and their surrogates is still prohibitively expensive. Especially for turbulent combustion models based on a particle LES/PDF approach, the CPU

*Corresponding author. Email: ps729@cornell.edu

cost and memory requirements of retaining the full species state vector to evaluate the chemical source term impose a low upper limit of the number of variables that can be used to describe the chemistry [1].

Adaptive chemistry approaches, which tailor the fidelity and size of the kinetic models used for reaction integration to the local flame conditions, have gained significant attention recently due to their ability to accurately describe the relevant combustion kinetics with significantly fewer variables and equations. The reduced mechanisms can be developed on-the-fly [2–4] or in an offline pre-processing stage [5–8]. The pre-partitioned adaptive chemistry (PPAC) [7] follows the latter approach: a set of reduced models is developed in an offline, pre-processing step by partitioning the composition space into several regions, and applying the DRGEP technique [9] in each of those regions using a sample composition database assumed to be representative of the composition space accessed at runtime. Those models are then dynamically selected and used in the actual CFD simulation based on local conditions. This technique has shown good performance in both partially stirred reactors (PaSR) [7, 10] and LES/PDF simulations [11]. However, in all cases, the performance metrics were defined in terms of the main combustion features: prediction of temperature and mass fractions of species directly involved in the hydrocarbon oxidation process. In this work, we further investigate the performance of PPAC, taken here as a representative of adaptive chemistry approaches, in accurately capturing both the main oxidation pathways and some secondary chemical process whose kinetics are driven by, but remain distinct from, the combustion itself. We take NO_x formation as a specific case study.

In DRGEP-based PPAC, the region-specific reduced kinetic mechanisms are obtained by ranking species and reactions by their importance in the prediction of a set of targets (e.g. species or heat release), and removing from the detailed mechanism those species and reactions deemed unimportant. Typical targets included to capture the main oxidation process are heat release, fuel, and some major products (CO_2) or radical (OH). Capturing the pathways associated with NO_x formation requires the addition of nitrogen-containing targets, the most obvious choices being NO and NO_2. We show in the following that when NO_x species are included in the set of targets, the DRGEP reduction procedure becomes overly conservative compared to the oxidation-only case, yielding region-specific reduced models much larger than one would expect for a given level of accuracy in targets prediction.

To address this issue, we propose a sequential approach to the generation of the region-specific kinetic models that leverages a new additive procedure for kinetic model reduction [12]. First the fuel oxidation pathways are identified in each region of the composition space using the original PPAC methodology, only including oxidation species as targets. This initial step is followed by selectively adding, directly at the reduced level, the appropriate NO_x reactions using the "building" algorithm recently developed by Heberle et al. [12].

This paper is organised as follows: the configurations and simulation frameworks used in the study, namely a partially stirred reactor and a CFD solver with LES/PDF capabilities are presented in Section 2, followed by a brief description of the two algorithmic components of this work: PPAC [7] and the building algorithm [12] in Section 3, and how those two components are integrated into the sequential procedure for region-specific reduced model development. The results of the two specific cases investigated as part of this work, a propane/air partially stirred reactor and a LES/PDF of Sandia Flame D are then presented and analysed in Section 4. Conclusions are provided in Section 5.

2. Numerical framework

Two numerical configurations are used in this work: a zero-dimensional partially stirred reactor, and a LES/PDF three-dimensional turbulent flame. A brief description of each that includes the most relevant information is provided here, the reader being referred to the cited work for additional details.

2.1. *Partially stirred reactor (PaSR)*

A PaSR represents a statistically spatially homogeneous flow-field with a constant number of particles evolving in time according to three distinct processes, or fractional steps: inflow/outflow, mixing, and reaction. In the inflow/outflow step, particles are selected randomly, and their compositions are replaced by fixed inflow compositions according to a user-specified residence time and stream mass flow rates. A pairwise mixing model is then used to partially mix compositions ($\phi^{(n)}$ and $\phi^{(n+1)}$ for particles n and $n+1$, respectively) between randomly chosen pairs of particles [13] based on a user-specified mixing time scale, τ_{mix}:

$$\begin{aligned} \frac{\mathrm{d}\phi^{(n)}}{\mathrm{d}t} &= -\frac{\phi^{(n)} - \phi^{(n+1)}}{\tau_{\text{mix}}} \\ \frac{\mathrm{d}\phi^{(n+1)}}{\mathrm{d}t} &= -\frac{\phi^{(n+1)} - \phi^{(n)}}{\tau_{\text{mix}}}. \end{aligned} \tag{1}$$

Finally, all compositions evolve in time due to reaction under adiabatic, isobaric conditions:

$$\frac{\mathrm{d}\phi^{(n)}}{\mathrm{d}t} = \boldsymbol{S}(\phi^{(n)}) \tag{2}$$

where $\boldsymbol{S}$ is the rate of change due to chemical reactions (or chemical source term) of composition $\phi^{(n)}$. A PaSR first goes through a transient stage for a few residence times before reaching a statistically stationary state. The PaSR implementation used in this work is described exhaustively in Liang et al. [7].

2.2. *LES/PDF flow solver*

The LES/PDF of Sandia Flame D is a hybrid mesh-particle method, which is performed here using the variable density low-Mach solver NGA [14]. The LES solver computes the filtered velocity field with second-order accurate discretization in space and time. The turbulent viscosity and diffusivity are computed using a Lagrangian dynamic subgrid-scale model [15].

For the reacting flows, a Lagrangian particle PDF method has been implemented in NGA [11] to solve for the one-point one-time joint density weighted filtered PDF of species mass fractions and enthalpy. In this approach, an equivalent particle system is designed to represent the PDF and its evolution. For each particle, a set of stochastic differential equations (SDE) is solved to account for particle transport, mixing, and reaction [16]. These SDEs are integrated using a simple first-order splitting method. The transport fractional step updates the particle position in physical space, the mixing fractional step handles changes occurring in particle compositions due to molecular mixing, and the reaction fractional step advances particle compositions to account for chemical reactions. The transport fractional step is performed using a simple forward Euler method. The mixing fractional

step uses the IEM model [17]. Finally the reaction fractional step is performed efficiently using a dynamic load balancing strategy [18].

The LES/PDF solver is two-way coupled, with the LES solver using a resolved density computed from the PDF solution. Additionally, the resolved composition from the PDF solver is used to compute the kinematic viscosity and molecular diffusivity. The resolved velocity field and turbulent diffusivity from the LES solver are used to advance the particle positions.

3. Methodology

Two key components are integrated in the proposed sequential approach for reduced model generation: the adaptive chemistry approach itself, and the additive methodology, referred to as the building algorithm below, used to identify the kinetics associated with the secondary pathways.

3.1. *Pre-partitioned adaptive chemistry (PPAC)*

PPAC [7] is tailored for particle PDF methods to simulate turbulent combustion systems, and consists of two stages: an offline pre-processing stage and the adaptive simulation stage. The pre-processing stage entails the generation of a set of reduced models, and the adaptive simulation stage selectively utilises those models during the reaction fractional step. The pre-processing stage consists of the following steps:

(1) **Database creation:** A database of compositions is assembled first using the detailed kinetic mechanism. The database is expected to be representative of the compositions likely to be encountered at runtime.
(2) **Partitioning:** Using this database and a cutting-plane algorithm, the composition space is partitioned into a user-specified number of regions, so that the compositions in each region are kinetically similar. The partition is stored conveniently in the form of a binary tree.
(3) **Generation of Reduced models:** A reduced kinetic model and its corresponding representation are then generated for each region using DRGEP, the compositions in the database belonging to that region, a set of user-specified targets, and an error cut-off parameter ε_c. The actual error is quantitatively measured *a-posteriori* by directly comparing reduced and detailed predictions of the targets and temperature:

$$\varepsilon = \max_{\mathcal{R}} \left(\frac{||\boldsymbol{Y}_{\boldsymbol{\mathcal{T}}}{}^{D}(\Delta t) - \boldsymbol{Y}_{\boldsymbol{\mathcal{T}}}{}^{R}(\Delta t)||_2}{||\boldsymbol{Y}_{\boldsymbol{\mathcal{T}}}{}^{D}(\Delta t)||_2}, \left| \frac{T^D(\Delta t) - T^R(\Delta t)}{T^D(\Delta t)} \right| \right) \tag{3}$$

where the maximum is taken over all particles in the database belonging to the region $\mathcal{R}$ under consideration, $\boldsymbol{Y}_{\boldsymbol{\mathcal{T}}}(\Delta t)$ and $T(\Delta t)$ are the targets mass fraction vector and the temperature after Δt, and the superscripts D and R refer to the use of detailed and reduced models, respectively.

During the actual simulation, the key steps through which a particle composition evolves in time are as follows:

(1) **Reconstruction:** Before the mixing fractional step, the detailed representation of the particle composition is reconstructed from its reduced skeletal representation.

(2) **Mixing:** In their detailed representation, the compositions are mixed following Equation (1).
(3) **Classification:** After mixing, each composition is classified into one of the regions using an efficient low-dimensional binary tree search algorithm.
(4) **Reduction:** Each particle composition is then converted to its reduced skeletal representation corresponding to the region it belongs to.
(5) **Integration:** The particle compositions in their reduced representations are then advanced in time due to reaction following Equation (2).

A full description of the PPAC algorithm is provided in [7].

3.2. *Building algorithm*

The building algorithm is a DRGEP-based iterative bottom-up approach to generate reduced kinetic mechanisms. Unlike the conventional graph-based reduction methods that rely on simulations using the detailed mechanisms to identify and remove unimportant species and reactions in a top-down fashion, the building algorithm follows an add-as-needed approach. Here the reduced mechanisms are progressively "built" with reactions selected from the detailed mechanism using a DRGEP-derived criterion in order to accurately predict the evolution of a set of user-defined targets, $\mathcal{T}$. Most importantly, this algorithm provides a framework to incrementally expand existing reduced models to accommodate a wider range of conditions, or to include new chemical pathways, such as NO_x chemistry in this work. A summary of the algorithm as used in this paper is provided here, with further implementation details available in Heberle et al. [12].

Let's consider a set of compositions, an initial reduced mechanism $\mathcal{M}_0$, a time interval Δt, a list of additional target species that were not accounted for in the original reduction $\mathcal{T}^B$, and a desired error cut-off parameter ε_c. The objective of the building process is to identify a minimal set of additional reactions required to properly capture the evolution of each composition over the time interval Δt within an error $\varepsilon < \varepsilon_c$. Since ε is an *a posteriori* measure, that is, it can only be calculated when the reduced mechanism is known, a surrogate criterion corresponding to a DRGEP coefficient cut-off, $\varepsilon_{\mathrm{DRGEP}}$, is used instead during the building process. $\varepsilon_{\mathrm{DRGEP}}$ is initialised to a large value. The steps are as follows:

(1) We define the edge of the mechanism $\mathcal{M}_0$, denoted by $\delta\mathcal{M}_0$, as the set of reactions from the detailed mechanism that satisfy one of the following conditions: (a) every reactant in the reaction is already present in $\mathcal{M}_0$, or (b) every product in the reaction is already present in $\mathcal{M}_0$. The union of $\mathcal{M}_0$ and $\delta\mathcal{M}_0$ is called the test mechanism ($\mathcal{M}_0^\star$).
(2) DRGEP reaction coefficients (as defined in [9]) are computed for all compositions using $\mathcal{M}_0^\star$ over the time interval Δt.
(3) Reactions in $\delta\mathcal{M}_0$ with a DRGEP reaction coefficient larger than $\varepsilon_{\mathrm{DRGEP}}$ are added to $\mathcal{M}_0$.

Steps 1-3 are repeated with the updated $\mathcal{M}_0$ until there is no reaction left in $\delta\mathcal{M}_0$ satisfying the criteria in step 3. At this point, the actual error metric ε is evaluated. If it is larger than ε_c, the process is restarted using a smaller $\varepsilon_{\mathrm{DRGEP}}$ in order to refine the resulting reduced model. The process stops when ε becomes smaller than ε_c.

3.3. *Additive treatment of secondary pathways in PPAC*

In the regular PPAC process (simply labelled "PPAC" below), the region-specific reduced models for a given ε_c are directly obtained using a single set of targets including both oxidation and nitrogen-related species. In contrast, when using the building algorithm to handle the secondary processes, the algorithm, labelled "PPAC-Additive" below, proceeds in two distinct stages, both done during pre-processing:

(1) **Reduction:** In the first stage, region-specific reduced models are generated according to the desired error cut-offs, but *using the oxidation targets only*.
(2) **Building:** In the second stage, starting from the oxidation-only reduced mechanisms, the building algorithm is applied using a set of targets relevant for the secondary processes only (e.g. NO, NO_2, and heat release). The second stage stops when all regions satisfy their error cut-off criterion, now defined based on the secondary set of targets.

The resulting region-specific models are then used in a similar way during the adaptive simulations. The next section quantifies in two different configurations the benefits of using the latter, 2-stage approach. To improve the treatment of PPAC-Additive, two additional modifications are performed compared to the original PPAC and building algorithm, discussed in the previous sections.

(1) **M1:** The first key modification is in the PPAC algorithm itself. The error cut-off parameter ε_c in the pre-processing stage of PPAC is combined with a scaling process similar to the one initially developed for DRGEP [9], to create a region-specific cut-off, which allows for greater model reduction in regions where the targets are less chemically active. The region-specific error cut-off ε_c^i for region i is defined as:

$$\varepsilon_c^i = \frac{\varepsilon_c}{\alpha_G^i} \quad \text{where} \quad \alpha_G^i = \frac{\langle \alpha_t^i \rangle_{t\in\mathcal{T}}}{\max_i \langle \alpha_t^i \rangle_{t\in\mathcal{T}}} \tag{4}$$

where α_t^i is the scaling coefficient of target t corresponding to the compositions that belong to region i [7, 9], and $\langle\cdot\rangle_{t\in\mathcal{T}}$ denotes the mean over the set of targets, $\mathcal{T}$. In essence, α_G^i is unity for the most important region for $\mathcal{T}$, and a lower than unity value of α_G^i results in an increase in ε_c^i, and therefore, more reduced models. Note that in PPAC-Additive, ε_c is set to the same value for both reduction and building stages. However, because the targets and their corresponding scaling coefficients are different in these stages, the values of region-specific ε_c^i do vary across regions and between the two stages.
(2) **M2:** The building algorithm is modified in PPAC-Additive from its original form [12] as described below:
   a. (a)In the building stage of PPAC-Additive, both species and reaction DRGEP coefficients are evaluated for $\mathcal{M}^\star$. Then reactions in $\delta\mathcal{M}_0$ with a DRGEP reaction coefficient larger than $\varepsilon_{\text{DRGEP}}$ and involving the species with the highest DRGEP coefficients are added to $\mathcal{M}_0$.
   b. (b)In contrast to the original building algorithm where $\varepsilon_{\text{DRGEP}}$ is set to a fixed value [12], $\varepsilon_{\text{DRGEP}}$ in PPAC-Additive is adjusted iteratively in each region until all reactions needed to bring the error below the corresponding region-specific error threshold ε_c^i have been added. Therefore, the cut-off parameter ε_c is the only parameter that needs to be specified by the user.

4. Results and discussion

4.1. *PaSR configuration*

The first configuration under consideration is a non-premixed piloted propane-air PaSR. The detailed propane mechanism used is that of Petersen et al. [19], with an added NO_x sub-mechanism [20], yielding a mechanism with 140 species and 1695 reactions. The PaSR parameters are those used in [7], with 100 particles and three inflow streams: pure fuel, air, and a burnt gas pilot. The PaSR is initially run for three residence times after which it reaches a statistically stationary state. 10,000 distinct compositions are then randomly sampled over the next 10 residence times to form the composition database. The number of regions is specified to be 10. The oxidation targets are the fuel, CO_2, CO, OH, and heat release, the nitrogen related targets being NO and NO_2.

First, we compare the error incurred in the prediction of the NO mass fraction and the temperature obtained during the adaptive simulation when using the region-specific models obtained with PPAC and PPAC-Additive, as a function of the relative number of species used in the kinetic models in each case. The incurred error for a quantity X is defined as:

$$\varepsilon_X = \frac{\sum_{k=1}^{n_t}\sum_{n=1}^{n_p}|X_k^{(n),A} - X_k^{(n),D}|}{\sum_{k=1}^{n_t}\sum_{n=1}^{n_p}|X_k^{(n),D}|}, \tag{5}$$

where n_t is the number of time steps and n_p, the number of particles. $X_k^{(n),A}$ and $X_k^{(n),D}$ represent the values of quantity X for particle n at the kth time step using the adaptive and detailed chemistry, respectively. The relative number of species used throughout the simulation is defined as:

$$n_{\text{rel}} = \frac{1}{n_t n_p n_s}\sum_{k=1}^{n_t}\sum_{n=1}^{n_p} n_{s,k}^{(n),A}, \tag{6}$$

where n_s is the number of species in the detailed model, and $n_{s,k}^{(n),A}$ is the number of species in the reduced model used by particle n at time step k. The comparison is shown in Figure 1.

For both model generation techniques, we observe, as expected, an increase in incurred error for both temperature and NO mass fraction as the relative number of species decreases, that is, as the region-specific models become more reduced. The temperature curves for both approaches are very similar, indicating that a similar level of reduction will yield a similar error in temperature prediction for both approaches. However, the trend is noticeably different when looking at NO prediction. At very low incurred error levels, corresponding to 80% of the species included on average in the region-specific models, the two methodologies do not show any notable difference. However, as the incurred error increases, the relative number of species required to reach a given error in the prediction of NO is observed to be significantly smaller in the PPAC-Additive case compared to the regular PPAC. For instance, to achieve a 3% error in NO mass fraction, PPAC (point '1' in in Figure 1) requires 75% of the detailed species, as opposed to only 56% for PPAC-Additive (point '2'): the model reduction done accounting for all targets at once, oxidation and NO_x formation, appears significantly less efficient at identifying reliably the dominant pathways necessary to predict NO formation.

Exploring this key observation further, n_{rel} is divided into two components: the relative number of oxidation species, $n_{\text{rel,Ox}}$, and nitrogen-containing species, $n_{\text{rel,NO}_x}$, both normalised by n_s. Those two numbers are plotted against ε_{NO} in Figure 2. In both approaches, $n_{\text{rel,NO}_x}$ turns out to be very similar, attributing the difference in n_{rel} observed in Figure 1

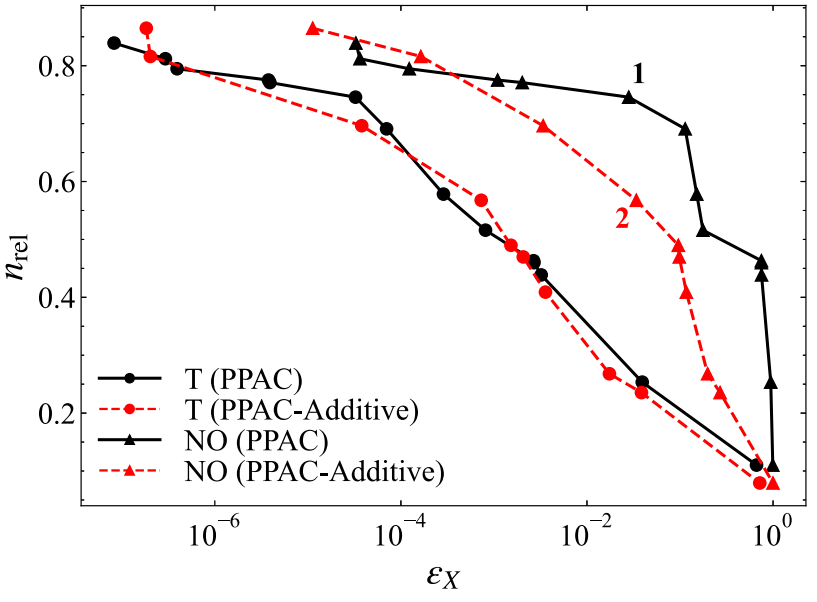

Figure 1. Relative number of species as a function of incurred error in temperature (circles) and NO mass fraction (triangles) for PPAC (black solid line) and PPAC-Additive (red dashed line) compared to the non-adaptive case. Points marked as '1' and '2' are used for further analysis in the text.

solely to an excess number of oxidation species selected by the regular, all-targets-at-once, reduction procedure.

During the reduction stage of PPAC, the unimportant species are removed according to their DRGEP species coefficients, which are calculated over all targets of interest. The results above provide evidence that conventional graph-based reduction methods that require users to specify a list of targets of interest do not optimally handle sets of targets associated with chemical pathways very different in nature, e.g. in this case, the primary pathways (fuel oxidation) and the pollutant formation (NO_x chemistry). When different targets are handled without distinction, unimportant oxidation species are added prior to the addition of important nitrogen-related species, their DRGEP species coefficients being lower and consequently appearing much later in the importance ranking. The additive procedure highlighted in this work effectively decouples primary and secondary targets, enabling a more selective identification of the species involved in the secondary process and its coupling to the primary combustion pathways.

Further region-specific analysis can be done by comparing the models corresponding to point '1' (PPAC) and '2' (PPAC-Additive), since both result in a similar incurred error. In particular, we can investigate the difference in the number of oxidation species retained in each region between those two cases, normalised by the number of oxidation species in the detailed mechanism. The results are plotted in Figure 3. The secondary y-axis shows the probability P_J of a particle to be classified to region J during the adaptive PaSR simulation. The kinetic model associated with Region 1, which is most frequently used ($\sim$ 50% of the particles) contains 18% more oxidation species when the additive process is not used and all targets are handled together, thus contributing the most to the difference observed in Figure 1. On the other hand, the kinetic model associated with Region 9,

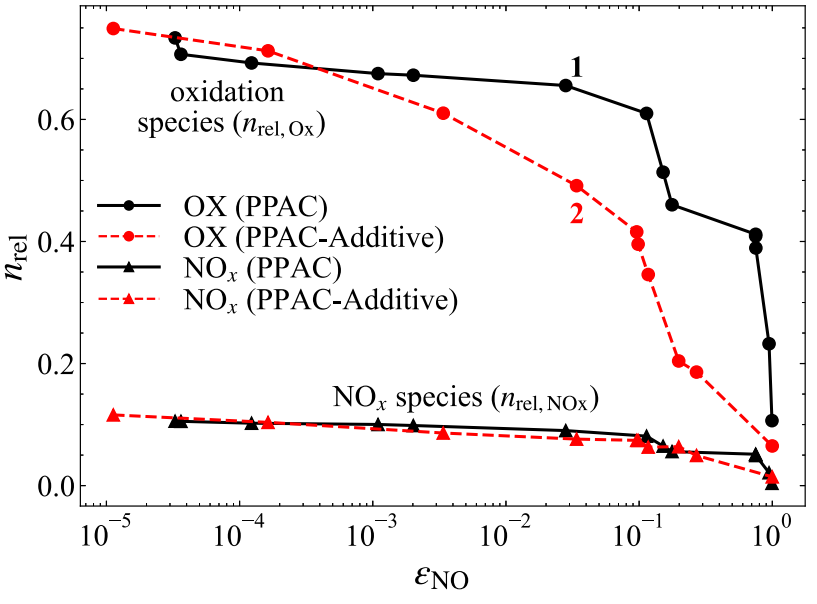

Figure 2. Relative number of oxidation ("OX" in legend) and NO_x species as a function of incurred error in NO mass fraction for PPAC and PPAC-Additive.

although containing the same number of oxidation species in both cases, is only used for 3% of the particles. Figure 4 shows the average wall clock time per time step relative to the detailed simulation. As a direct result of the difference in the number of species retained, the additive procedure for the generation of the reduced models also significantly impacts the CPU cost of the adaptive simulations, with for example, a 23% reduction in wall clock time per time step between PPAC-Additive ('2') and the regular PPAC ('1').

Finally, to emphasise the importance of the modifications M1 and M2 mentioned in Section 3.3, the same PasR simulations are run using PPAC-Additive without those modifications, which we label PPAC-Additive-No-Mods in the following. We compare the error incurred in the predictions of temperature and NO mass fraction for PPAC, PPA-Additive, and PPAC-Additive-No-Mods as a function of n_{rel} in Figure 5. As expected, we observe that PPAC-Additive-No-Mods requires significantly larger models to achieve the same level of accuracy compared to the original PPAC-Additive. Indeed, without M1, all targets are considered equally active and important, forcing the algorithm to retain their associated production and consumption pathways even when those can safely be neglected (e.g. fuel decomposition pathways in regions associated with post-flame chemistry). In addition, M2 provides a more sequential, and therefore more discriminating process to add reactions to the models, which is shown to be quite effective.

4.2. *LES/PDF of sandia flame D*

The additive reduction approach is next assessed in the context of LES/PDF with the simulation of Sandia Flame D [21]. The cylindrical configuration is 60D and 20D in the axial and radial directions, respectively. A non-uniform 192 (axial) × 140 (radial) × 32 (azimuthal) mesh is used. The mixing model constant is specified to be 4, and the number of particles per cell is chosen to be 25 [11]. GRI Mech 2.11 [22] with 48 species and 554

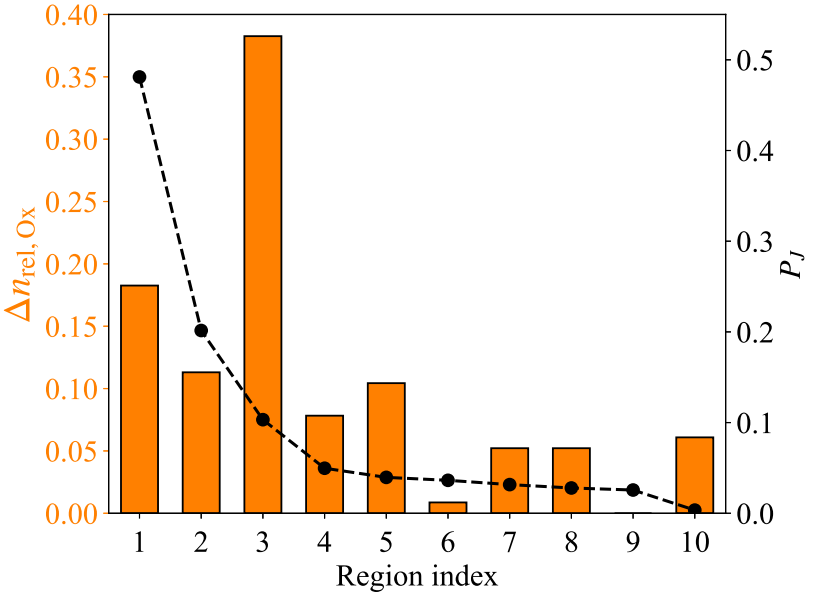

Figure 3. Region-specific difference in the number of oxidation species retained by the PPAC and PPAC-Additive reduction procedures, corresponding to an equivalent incurred error in the adaptive simulation. The circles indicate the probability of a particle to be in region J, P_J.

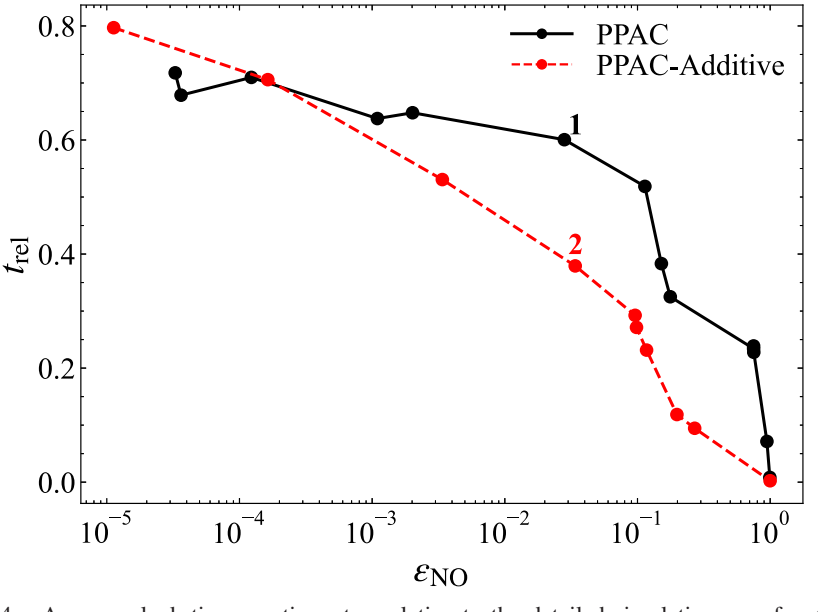

Figure 4. Average clock time per time step relative to the detailed simulation as a function of incurred error in NO mass fraction for PPAC and PPAC-Additive.

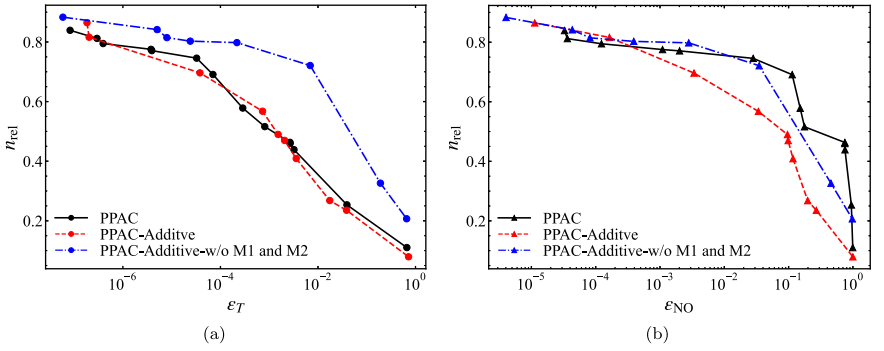

Figure 5. Relative number of species as a function of incurred error in (a) temperature, and (b) NO mass fraction for PPAC (black solid line), PPAC-Additive (red dashed line) and PPAC-Additive without modifications M1 and M2, compared to the non-adaptive case.

reactions is used for these computations. To accelerate the LES/PDF calculations, in-situ adaptive tabulation (ISAT) [13] is used in all LES/PDF runs. The ISAT tolerance is specified to be 10^{-4}, and the maximum table size is set to 500 MB for the detailed mechanism. During the adaptive simulation, the region-specific ISAT tables are allowed to reach a maximum size of 50 MB. The additional error introduced by ISAT is assumed to be negligible compared to the error introduced by the chemical reduction itself.

As the focus of this work is the performance of the additive reduction procedure in handling NO_x formation in an adaptive chemistry LES/PDF simulation, the composition database for the partitioning and reduction is obtained by down-sampling the composition particles obtained from an instantaneous snapshot of the detailed LES/PDF of the Sandia Flame D itself. The targets and number of regions are the same as for the PaSR case, and the partitions and region-specific kinetic models of varying levels of reduction are obtained in a similar fashion as above, using methane oxidation and nitrogen targets together (PPAC) or first using methane oxidation targets only, followed by the addition of reduced NO_x pathways using the building algorithm (PPAC-Additive). The incurred errors for the LES/PDF cases are obtained from Equation (5) by integrating the database compositions over 50 time steps using the detailed mechanism as reference. The incurred error in temperature and NO mass fraction as a function of the relative number of species used is plotted in Figure 6

Similarly to Figure 1, the results clearly show that for a given incurred error in NO mass fraction, the additive procedure yields smaller region-specific models. Figure 7, which breaks down the number of species into oxidation and nitrogen-containing species, confirms again that the difference in reduced model sizes comes primarily from an excessive number of oxidation species selected when oxidation and NO_x targets are handled together.

Two full-scale Sandia D flames are then simulated using the sets of models obtained with PPAC and PPAC-Additive generating less than 0.5% incurred error in NO mass fraction (Point '1' for PPAC and point '2' for PPAC-Additive in Figure 6). Note that in the PaSR case, the points corresponding to PPAC and PPAC-Additive were chosen based on a 3% error level (Figure 1). That incurred error was evaluated over multiple residence times involving both reaction and mixing in a PaSR. In contrast, the error evaluation in Figure 6 is more sensitive as it involves integrating the chemical source terms over a significant amount of time without any stabilising mixing processes. This extra sensitivity is

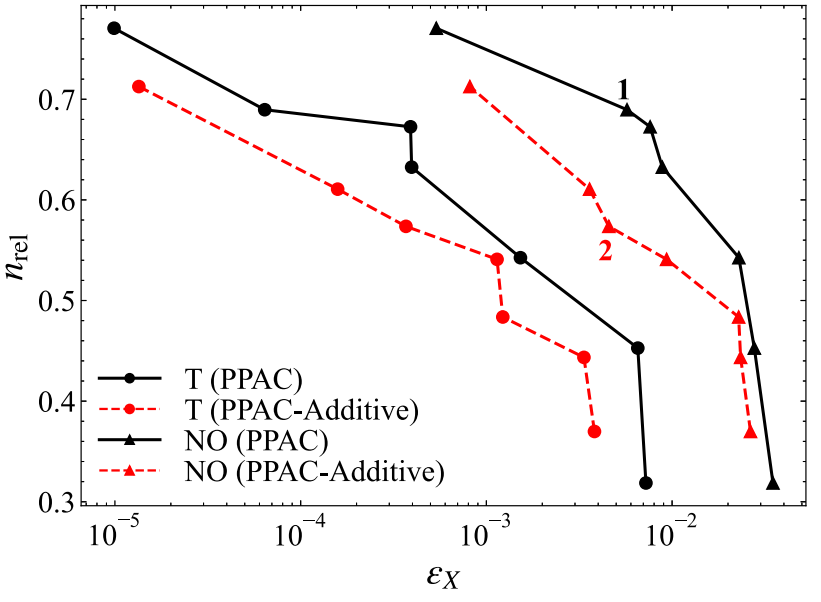

Figure 6. Relative number of species as a function of incurred error in temperature (circles) and NO mass fraction (triangles) for PPAC (black solid line) and PPAC-Additive (red dashed line) compared to the non-adaptive case. Point '1' and '2' are chosen for the full scale Sandia D runs from PPAC and PPAC-Additive, respectively.

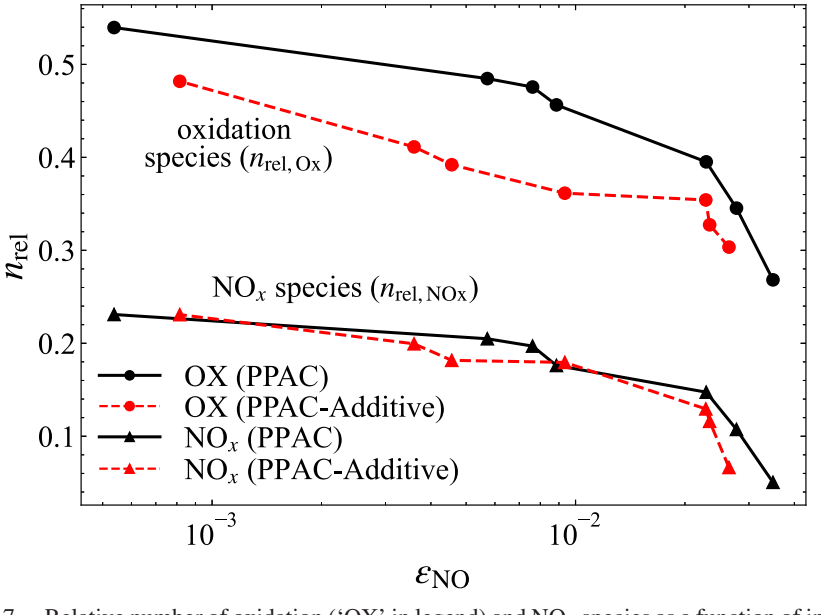

Figure 7. Relative number of oxidation ('OX' in legend) and NO_x species as a function of incurred error in NO mass fraction for PPAC and PPAC-Additive.

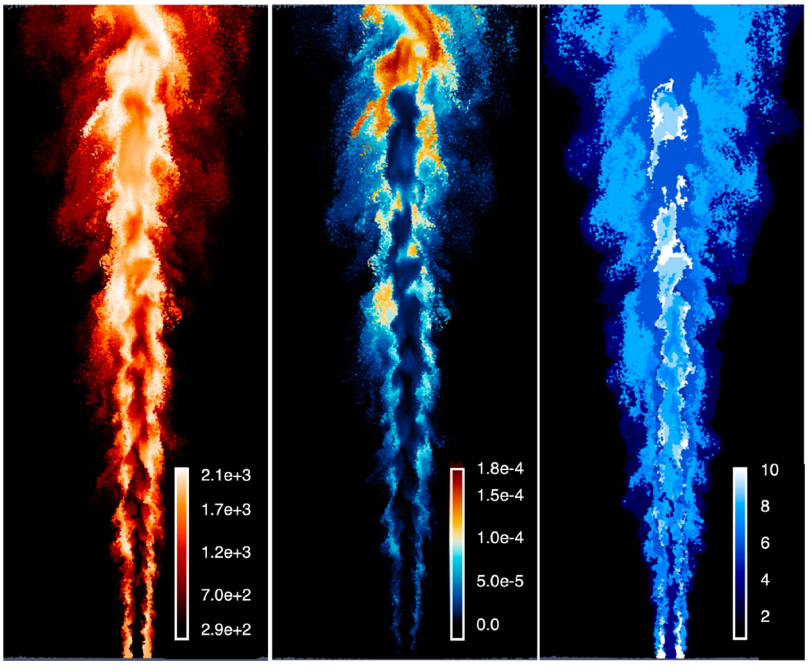

Figure 8. Instantaneous particle distribution coloured by temperature (left), NO mass fraction (middle) and index of the model used for reaction source term integration (right).

accounted for by choosing a smaller error cut-off for the selection of the reduced kinetic models, so that the overall LES/PDF error evaluated on average species and temperature profiles is of the order of a few per cent. Figure 8 shows the instantaneous particle distribution for the PPAC-Additive (or PPAC)-ISAT LES/PDF simulation coloured with temperature on the left and NO mass fraction in the middle. The right panel shows the same particle distribution coloured with the index of the reduced kinetic model used by the corresponding particle for the chemical source term integration. Figures 9(a ,b) show a break down of the number of oxidation and NO_x species in each of the models for PPAC and PPAC-Additive, respectively, using the same colour map as the right panel of Figure 8.

We observe that the particles in the co-flow region use the reduced model involving the smallest number of species for both PPAC and PPAC-Additve (model 1). The maximum NO mass fraction pockets coincide with regions of higher temperature across the flame brush. These regions can be attributed to the thermal route of NO formation, which is clearly the most important NO_x pathway in Sandia Flame D. Additionally, most of the particles in these high temperature pockets are integrated by model 6, which includes the chemistry associated with interaction of N_2 species with O or OH, important in NO formation. In case of both model 1 and 6, which are the two most used models in the LES/PDF runs, PPAC models contain 35% more oxidation species than PPAC-Additive models, respectively (Figure 9). On the other hand, the prompt NO pathways, which are dominated by the production of HCN from CH (Fenimore mechanism), are mostly covered by models 5 and 9. The regions with maximum N_2O mass fraction coincide with particles using model 8, which covers the less important N_2O-related pathways. The other models with high NO_x species observed in Figure 9 share both thermal and prompt NO pathways.

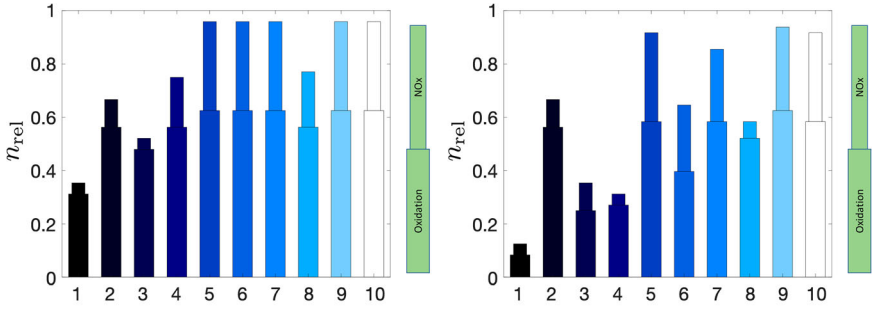

Figure 9. Relative number of oxidation and NO_x species in each model with respect to the detailed mechanism for (a) PPAC, and (b) PPAC-Additive. The colour pattern matches that of the right panel of Figure 8.

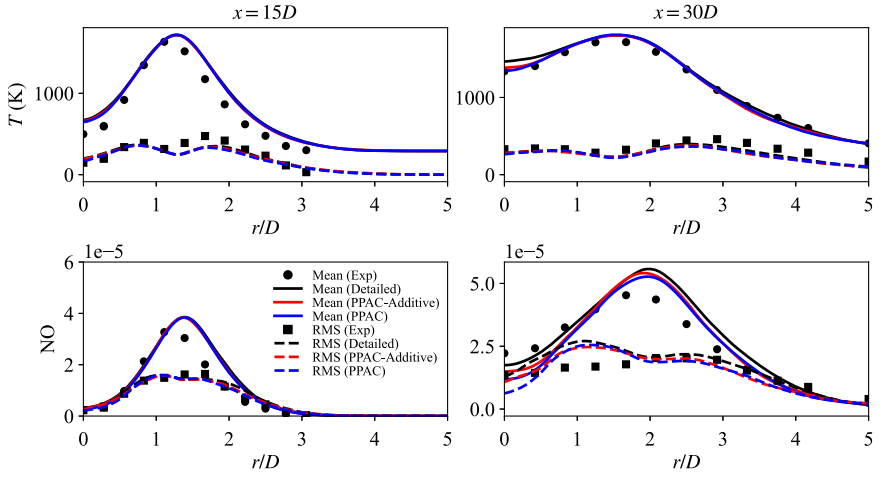

Figure 10. Comparison of radial profile of the experimental (Exp) and the computed (Detailed, PPAC and PPAC-Additive) resolved mean and RMS of temperature and NO mass fraction at two different axial locations: 15D and 30D.

Finally, the models with the fewer number of nitrogen-containing species are primarily used near the fuel jet core and in the surrounding area of the flame, where the temperature is low. Overall, the PPAC run utilises approximately 18% more relative number of species (Equation (6)) than PPAC-Additive for the reaction fractional step over two flow-through times, resulting in a 5% reduction in wall clock time per time step for the latter. Note that consistent with the PaSR results presented above, the speed-up is expected to increase considerably when dealing with larger kinetic mechanisms due to the combined effect of a much higher potential for reduction (methane combustion can be described in detail with less than 50 species only) and an increasing fraction of the computational time spent in chemistry-related calculations during the LES/PDF simulation.

Figure 10 compares the radial profiles of the resolved mean and RMS of temperature and NO mass fraction obtained from the detailed, PPAC-Additive and PPAC simulations at two different axial locations, 15D and 30D from the burner exit (D is the burner diameter). Statistics have been collected for two flow-through times. To quantify the difference

between the adaptive (PPAC-Additive or PPAC) and detailed simulations, we use the normalised root mean square difference (RMSD) [23], defined as:

$$\mathcal{E}(\xi) = \frac{\left[\xi^{\mathrm{A}} - \xi^{\mathrm{D}}\right]_{rms}}{\xi_{\mathrm{ref}}}, \tag{7}$$

where ξ^{A} and ξ^{D} denote the quantities obtained from adaptive and detailed simulation, respectively, ξ_{ref} is the reference value of each quantity of interest. ξ^{ref} is considered to be 1000K for temperature, and the maximum NO mass fraction among all the radial profiles at both axial locations: $15D$ and $30D$. The $[\cdot]_{rms}$ is computed over all the radial locations at all the considered axial locations. We observe that as expected, there is no significant difference between the adaptive simulations, with the RMSD values of resolved mean and RMS of temperature and NO mass fraction remaining below 3% and 5% of the detailed simulation from both PPAC-Additive and PPAC simulations, respectively.

5. Conclusions

A new approach for the generation of reduced chemistry models describing distinct, but coupled chemical processes such as fuel oxidation and NO_x formation has been presented in the context of an adaptive chemistry approach. It relies on a sequential approach, in which reduced models for the primary kinetic process are first developed, followed by a selective addition, directly at the reduced level, of the reactions necessary to capture the secondary chemistry process up to a user-level error tolerance. The procedure has been assessed for NO_x formation in two different configurations: a propane/air PaSR and a LES/PDF of Sandia Flame D. The additive approach was found to be much more selective in identifying the most important reactions pertaining to the secondary process, compared to a traditional reduction approach where targets from both chemical processes are handled simultaneously. The difference between both approaches can be attributed nearly exclusively to an excess number of oxidation species in the traditionally reduced models that are not related to the NO_x formation, and not necessary for the proper prediction of the main oxidation pathways.

Disclosure statement

No potential conflict of interest was reported by the author(s).

Funding

This material is based upon work supported by NSF [award number CBET-1653609].

ORCID

Pushan Sharma http://orcid.org/0000-0001-9670-7147
Perrine Pepiot http://orcid.org/0000-0001-9870-2809

References

[1] Pope S.B., Small scales, many species and the manifold challenges of turbulent combustion, Proc. Combust. Inst. 34 (2013), pp. 1–31.
[2] Liang L., Stevens J.G., and Farrell J.T., A dynamic adaptive chemistry scheme for reactive flow computations, Proc. Combust. Inst. 32 (2009), pp. 527–534.

[3] Ren Z., Liu Y., Lu T., Lu L., Oluwole O.O., and Goldin G.M., The use of dynamic adaptive chemistry and tabulation in reactive flow simulations, Combust. Flame 161 (2014), pp. 127–137.
[4] Yang S., Ranjan R., Yang V., Menon S., and Sun W., Parallel on-the-fly adaptive kinetics in direct numerical simulation of turbulent premixed flame, Proc. Combust. Inst. 36 (2017), pp. 2025–2032.
[5] Banerjee I. and Ierapetritou M.G., An adaptive reduction scheme to model reactive flow, Combust. Flame 144 (2006), pp. 619–633.
[6] Schwer D.A., Lu P., and Green Jr W.H., An adaptive chemistry approach to modeling complex kinetics in reacting flows, Combust. Flame 133 (2003), pp. 451–465.
[7] Liang Y., Pope S.B., and Pepiot P., A pre-partitioned adaptive chemistry methodology for the efficient implementation of combustion chemistry in particle pdf methods, Combbust. Flame 162 (2015), pp. 3236–3253.
[8] D'Alessio G., Parente A., Stagni A., and Cuoci A., Adaptive chemistry via pre-partitioning of composition space and mechanism reduction, Combust. Flame 211 (2020), pp. 68–82.
[9] Pepiot P. and Pitsch H., An efficient error-propagation-based reduction method for large chemical kinetic mechanisms, Combust. Flame 154 (2008), pp. 67–81.
[10] Newale A.S., Liang Y., Pope S.B., and Pepiot P., A combined PPAC-RCCE-ISAT methodology for efficient implementation of combustion chemistry, Combust. Th. Mod. 23 (2019), pp. 1021–1053.
[11] Newale A.S., Pope S.B., and Pepiot P., Computationally-efficient and accurate particle pdf simulations of turbulent combustion using coupled pre-partitioned adaptive chemistry and tabulation. Proc. Combust. Inst 38 (2020), pp. 2721–2729.
[12] Heberle L., Sharma P., and Pepiot P., Automated construction of reduced mechanisms and additive reaction modules, Combust. Flame 234 (2021), pp. 111682.
[13] Pope S.B., Computationally efficient implementation of combustion chemistry using in situ adaptive tabulation. Combust. Th. Mod (1997), pp. 41–63.
[14] Desjardins O., Blanquart G., Balarac G., and Pitsch H., High order conservative finite difference scheme for variable density low mach number turbulent flows, J. Comp. Phys. 227 (2008), pp. 7125.
[15] Meneveau C., Lund T.S., and Cabot W.H., A lagrangian dynamic subgrid-scale model of turbulence, J. Fluid Mech. 319 (1996), pp. 353–385.
[16] Wang H. and Pope S.B., Large eddy simulation/probability density function modeling of a turbulent $CH_4/H_2/N_2$ jet flame, Proc. Combust. Inst. 33 (2011), pp. 1319–1330.
[17] Villermaux J. and Devillon J., Représentation de la coalescence et de la redispersion des domaines de ségrégation dans un fluide par un modèle d'interaction phénoménologique, Proc. Int. Symp. Chem. Reac. Eng. 26 (1972), pp. 1–13.
[18] Gruselle C., *Etude du développement d'une flamme soumise à un gradient de concentration: Rôle de la stratification et des EGR*, Ph.D. diss., INSA de Rouen, 2014
[19] Petersen E.L., Kalitan D.M., Simmons S., Bourque G., Curran H.J., and Simmie J.M., Methane/propane oxidation at high pressures: Experimental and detailed chemical kinetic modeling, Proc. Combust. Inst. 31 (2007), pp. 447–454.
[20] Zhang Y., Mathieu O., Petersen E.L., Bourque G., and Curran H.J., Assessing the predictions of a NOx kinetic mechanism on recent hydrogen and syngas experimental data, Combust. Flame 182 (2017), pp. 122–141.
[21] Barlow R. and Frank J., Effects of turbulence on species mass fractions in methane/air jet flames, Symp. Int. Combust. 27 (1998), pp. 1087–1095.
[22] Bowman C., Hanson R., Davidson D., Gardiner J.W.C., Lissianski G.S.V., Golden D., Frenklach M., and Goldenberg M., *Gri-mech 2.11*, http://www.me.berkeley.edu/gri_mech/ (1995)
[23] Hiremath V., Lantz S.R., Wang H., and Pope S.B., Large-scale parallel simulations of turbulent combustion using combined dimension reduction and tabulation of chemistry, Proc. Combust. Inst. 34 (2013), pp. 205–215.